INTEGRAL Observations of the Galactic 511 keV Emission and MeV Gamma-ray Astrophysics

K. Watanabe

NASA Goddard Space Flight Center & Univ. of Maryland College Park, USA

On behalf of the INTEGRAL/SPI Science Team

Abstract

Although there are a number of interesting phenomena, such as Nucleosynthesis in stars, in the MeV energy region, the observations have been difficult due to a small signal to noise (background) ratio (<1%). While NASA's Compton Gamma-ray Observatory (CGRO) enabled us to explore the Gamma-ray universe, ESA's INTEGRAL mission, launched in 2002, is providing us more detailed information with its superior energy and angular resolution. We will briefly discuss some of the current issues in MeV Gamma-ray Astrophysics. Then, we will focus on the Galactic 511 keV emission with the latest INTEGRAL observations, and talk about challenges we currently have.

1. The MeV Gamma-ray Astrophysics

Some of major Gamma-ray lines in the MeV energy region we are interested in the most include the ^{26}Al line at 1.809MeV, the ^{60}Fe lines at 1.172 & 1.333MeV, the ^{44}Ti line at 1.156MeV due to Nucleosynthesis in massive stars, the decay line from ^{56}Co to ^{56}Fe at 0.847 & 1.238 MeV in Supernovae, the Neutron-Proton recombination line at 2.223 MeV in Neutron star binaries (Bildsten, Salpeter & Wasserman 1993), the^{12}C excitation line at 4.439 MeV and the^{16}O excitation line at 6.129 MeV due to Cosmic Ray interactions. Studies of Gamma-Ray Bursts, Hypernovae, Black Holes, Pulsars, Solar Flares, AGNs, and Cosmic Gamma-ray Background in this energy range have also revealed many new facts. The biggest problem is, however, that the signal to noise (background) ratio is so small (< 1%). Thus, very detailed background studies must be carried out. We will discuss briefly some of them as follows.

1.1 ^{26}Al

The ^{26}Al line at 1.809MeV was first detected by HEAO-C (Mahoney et al. 1984). It is narrowly confined to the Galactic Plane with local hot spots in the Cygnus and Vela regions [Fig. 1, also see CGRO/COMPTEL (Diehl et al. 1995; Knödlseder et al. 1999)]. Although a broadened line (5.4 ± 1.4 keV FWHM) was reported [GRIS (Naya et al. 1996)], no further evidence has been reported [RHESSI (Smith 2004), INTEGRAL (Diehl et al. 2003)]. The recent INTEGRAL/SPI observation of the Cygnus region, where young stars and WR stars dominate, shows a little broader width than that on Inner Galaxy (Fig.2).

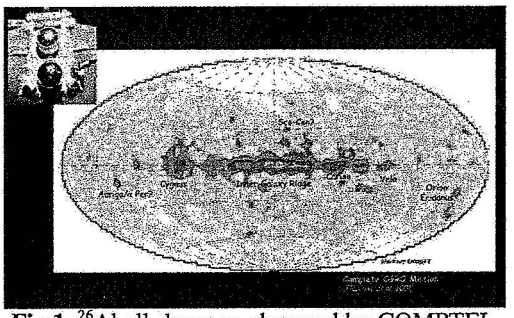

Fig.1 ^{26}Al all sky map observed by COMPTEL (Plüschke et al., 2001)

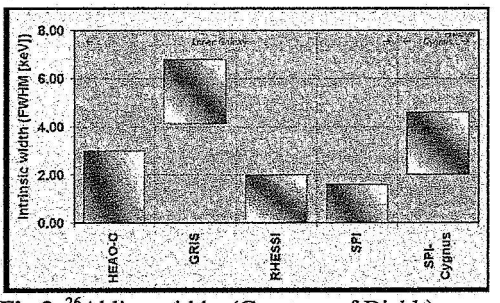

Fig.2 ^{26}Al line widths (Courtesy of Diehl)

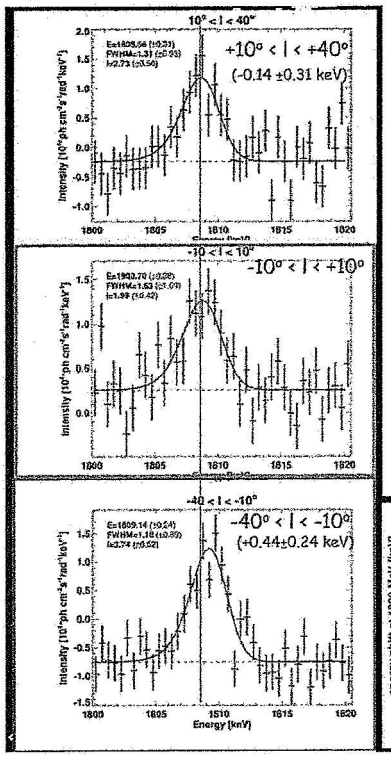

Galactic rotation affects the peak energy of the spectrum. The Doppler shift of the centroid has been observed by SPI. The three left panels in Fig. 3 illustrate these shifts. The upper panel is a red shift (0.14±0.31keV) at the galactic longitude between +10° and +40° and the bottom panel is a blue shift (0.44±0.24keV) at between -10° and -40°. The middle panel with no spectrum shift is at the galactic center. The right bottom panel shows the energy shifts as function of the galactic longitudes with indication of the three data of the left panels. The sources are not localized. We calculate the total galactic mass of ^{26}Al = 2.8 (±0.8) Mo. Although we observe a small line broadening from Inner Galaxy (the middle panel in Fig. 3), the change is within the errors, hence, not significant.

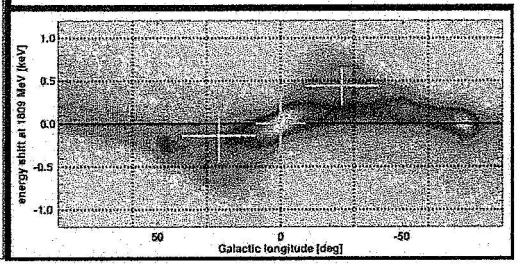

Fig.3 ^{26}Al spectrum centroid shifts due to the Galactic Rotation . (Courtesy of Diehl)

1.2 ^{60}Fe

As shown in Fig. 4 (left: RHESSI, Smith, 2004, right:SPI, Harris et al., 2005) the ^{60}Fe lines at 1.172 & 1.333 MeV have been marginally detected. The observed fluxes are $3.6\pm1.4 \times 10^{-5}$ ph cm^{-2}s^{-1} with 2.6σ detection (RHESSI) and $4.0\pm1.3 \times 10^{-5}$ ph cm^{-2} s^{-1} with 3σ (SPI). Thus, they are comparable. The ^{60}Fe/^{26}Al ratio in the Galaxy is 0.11 ± 0.03 (Harris et al. 2005). Theoretical models of SNII, however, predict the ratio being near unity (Limongi & Chieffi, 2003, also see Fig.5). These observations indicate that some other source of ^{26}Al besides explosive nucleosynthesis in core-collapse SNe are required.

1.3 Cosmic Gamma-ray Background (CGB)

Fig. 6 summarizes the CGB observations made by several different space missions. In the MeV region both CGRO/COMPTEL (Kappadath, et al. 1996) and SMM (Watanabe et

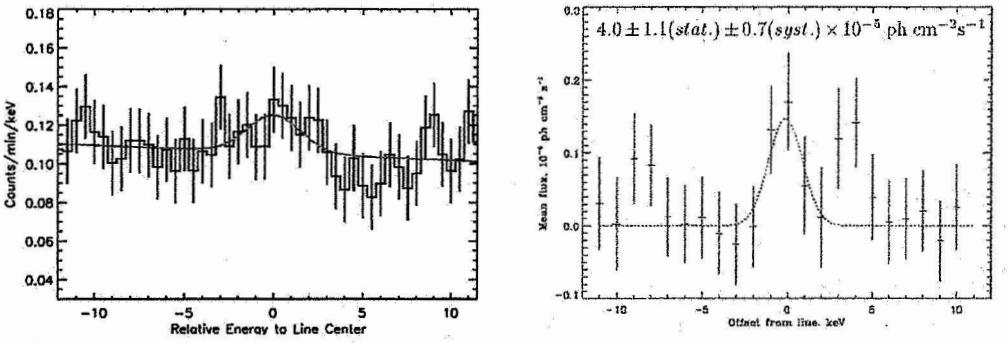

Fig.4 ^{60}Fe observations by RHESSI (left, Smith, 2004) and SPI (right, Harris et al.,2005)

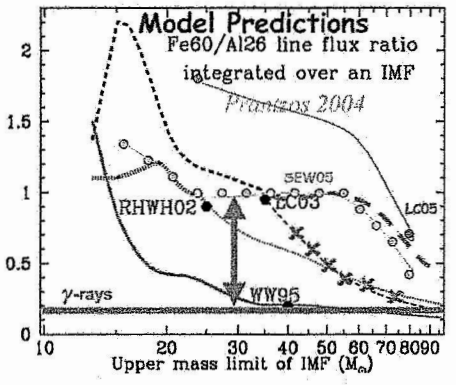

Fig.5 Theoretical predictions of the galactic ^{60}Fe/^{26}Al ratio (Prantzos, 2004)

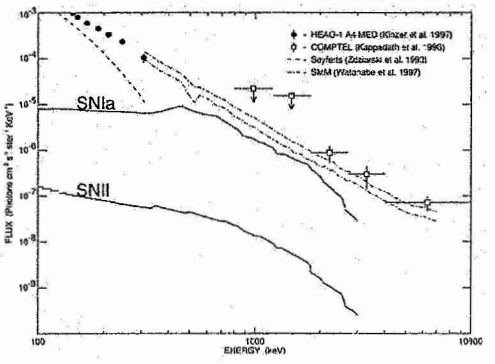

Fig.6 The CGB observations and SNIa contribution. (Watanabe, et al., 1999)

al., 1997) results show a power-law spectra. Seyfert galaxies seem to be responsible for the energies < ~300keV (Zdziarski, et al., 1993) and, the decay chain of ^{56}Ni => ^{56}Co => ^{56}Fe in the cosmological SNIa could produce the CGB flux comparable to the observed one (Watanabe, et al., 1999). Some recent studies (e.g. Zhang et al. 2004), however, demonstrate that SNIa could contribute only ~1% of the CGB flux due to uncertainties of the SNIa rates and the star formation rates. Some suggest (e.g. Ahn, et al., 2005) a Dark Matter scenario. Since there are many unknowns, we need to await future Gamma-ray missions, such as Advanced Compton Telescope (ACT), to conclude the origin(s).

2. INTEGRAL Mission

INTEGRAL (INTErnational Gamma-Ray Laboratory) is an ESA (European Space Agency) mission launched on October 17th, 2002. Its mission science is Gamma-ray astronomy in the energy range from 15 keV to 10 MeV The payload includes two main instruments: SPI (germanium spectrometer) and IBIS (CdTe + CsI) imager, as well as two monitor Instruments: JEM-X (x-ray monitor) and OMC (optical monitor). This mission has significant improvements in performance over Compton Gamma-Ray Observatory (CGRO) with new technologies. For instance, Germanium detectors and CdTe detectors have ~ 50 times better energy resolution and ~ 15 times better angular resolution than CGRO, respectively. INTEGRAL forms complementary set with SWIFT (gamma-ray bursts) and GLAST (high-energy gamma-rays). Fig. 7 – Fig. 10 illustrate the

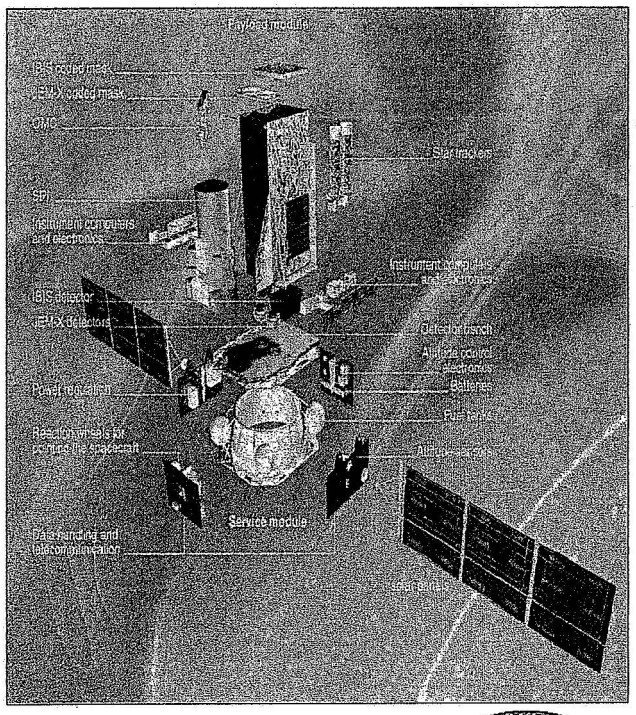

Fig.7 INTEGRAL space craft

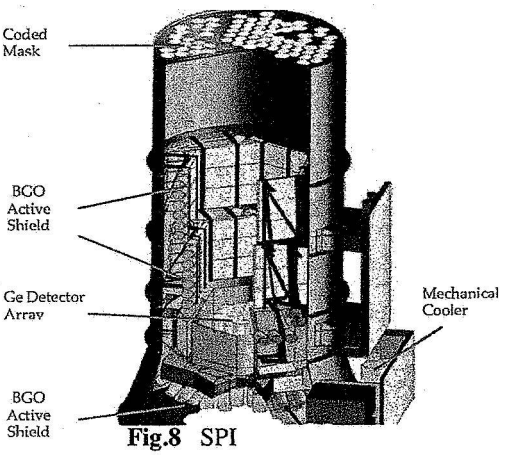

Fig.8 SPI

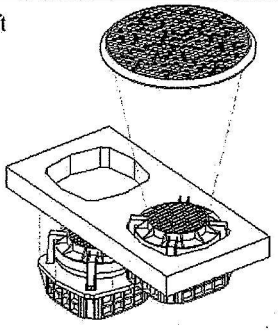

Fig.9 JEM-X

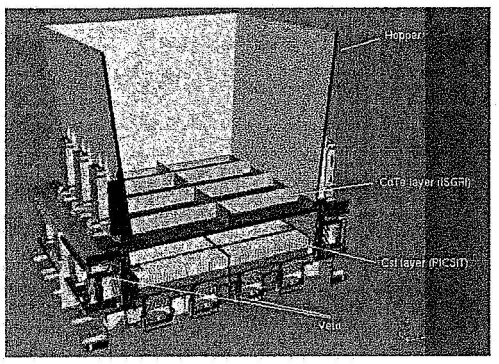

Fig.10 IBIS

space craft, SPI, JEM-X, and IBIS. Table 1 summaries the characteristics of these detectors.

SPI, IBIS, and JEM-X employ coded aperture imaging. Since Gamma-rays can not be focused easily, INTEGRAL uses the coded mask technique. It is basically a pinhole

	Energy Range	**Energy Resolution**	**Field of View**	**Angular Resolution**	**Detector Area**
SPI(Spectrometer on INTEGRAL	18 keV - 8 MeV	2.2keV @1.3MeV	16 deg fully coded	2.5 deg FWHM	500 cm^2 (19 hexagonal Ge detectors)
IBIS (Imager on Board the Integral Satellite)	15 keV - 10 MeV	8%@100keV 10%@1MeV	8.3 x 8.0 deg fully coded	12 arcmin FWHM	2600 cm^2(4x4x2 mm CdTe pixels)ISGRI, 3000 cm^2 (9x9x30 mm CsI pixels)PICsIT
JEM-X (Joint European X-ray Monitor)	3-35keV	1.3keV @10keV	4.8deg fully coded	3 arcmin	500 cm^2 (2 imaging microstrip gas chambers (90% Xenon + 10% Methane)

Table 1 Characteristics of each detector

camera with many holes. Incoming Gamma-rays from sources come into detectors through the coded-masks (see Fig.11). Then, the detectors can be deconvolved allowing us to separate and locate individual sources, and create images.

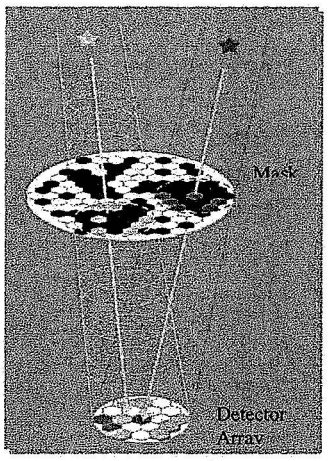

Fig. 11 Coded Aperture Imaging

INTEGRAL has made many discoveries of various new sources. They include High Mass X-ray Binaries (HMXB):IGR J16318-4848, IGR J16320-4751, IGR J17391-3021, Seyfert Galaxy: IGR J18027-1455, Low Mass X-ray Binaries (LMXB):IGR J16358-4726, IGR J16418-4532, IGR J17464-3213, Neutron Star: IGR J17597-2201, Gamma-ray sources: IGR J00291+5934, IGR J06074+2205, IGR J07597-3842, IGR J11305-6256, IGR J16167-4957, IGR J16479-4514, IGR J16558-5203, IGR J17252-3616, IGR J18325-0756, IGR J18450-0435,IGR J18483-0311, and IGR J21247+5058.

Some recent accomplishments are: a discovery of a faint persistent source within 1' of Sgr A* (Bélanger et al., 2005), an identification of the Galactic TeV (H.E.S.S.) sources: IGRJ18135-1751 (Ubertini et al.,2005) & AX J1838.0-065 (Malizia et al., 2005), detection of fast X-ray transients of just a few hours duration: XTE J1739-302 (Sguera et al.,2005; Smith et al., 2005), discoveries of the fastest known accreting X-ray milli-second pulsar IGR J00291+5934(1.67ms, P_{orb}= 2.46h) (e.g. Falanga et al., 2005), and Anomalous X-ray Pulsar 4U0142+614 (den Hartog et al., 2004). Gamma-Ray Bursts or X-ray flashes have been also detected (e.g. GCN #3059, 3323, 3348, 3430, 3446, 3472, 3552, 3607, 4002, 4007, 4192).

3. The Galactic 511 keV Emission

3.1 Possible Positron Sources

Although no positron sources have been identified yet, there are a several possible sources. In massive stars (e.g. Wolf-Rayet) positrons can be created by nucleosynthesis in stellar interior. They are convected to the surface and will be transported into interstellar medium (ISM) by stellar winds. Hypernovae, which are asymmetric explosions of a massive (> 30 M_{sun}) stars, are another possibility. Positrons can be efficiently transported outward by strong jets and escape into low optical depth regions where they subsequently annihilate. Pair plasmas are believed to exist in Black Holes (BH) jets. Positrons could either be aggregate emission from many BHs in Galactic Center region or from a single massive BH at Galactic Center. Beta-decay of radioactive nuclei created in type Ia supernovae explosion also produces positrons, and they are transported into ISM in expanding shell. There has been recent speculation on the possible existence of light (mc^2 < 100 MeV) dark matter particles which would decay or annihilate primarily through the formation of electrons and positrons. A tangle of light superconducting strings in the Milky Way also could create positrons. In this scenario the positron production is proportional to the Galactic magnetic field.

3.2 511 keV Spectroscopy

The measured 511 keV line energy is consistent with the rest energy of mc^2 = 511.00 keV. The narrow line width (2.3 keV) is also consistent with annihilation in warm interstellar clouds (see Table 2). A step is seen in continuum from ortho-positronium. (Fig.11).

511 keV Line Flux (10^{-3} cm^{-2} s^{-1})	*1.35 ± 0.11*
Line Energy (keV)	*511.14 ± 0.08*
FWHM (keV)	*2.34 ± 0.24*
Positronium Continuum Flux (10^{-3} cm^{-2} s^{-1})	*4.7 - 10.2*
Ps fraction	*> 0.88*

Table 2 Line characteristics.

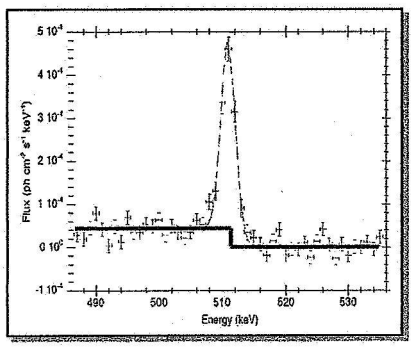

Fig. 11 Observed 511 keV line spectrum by SPI

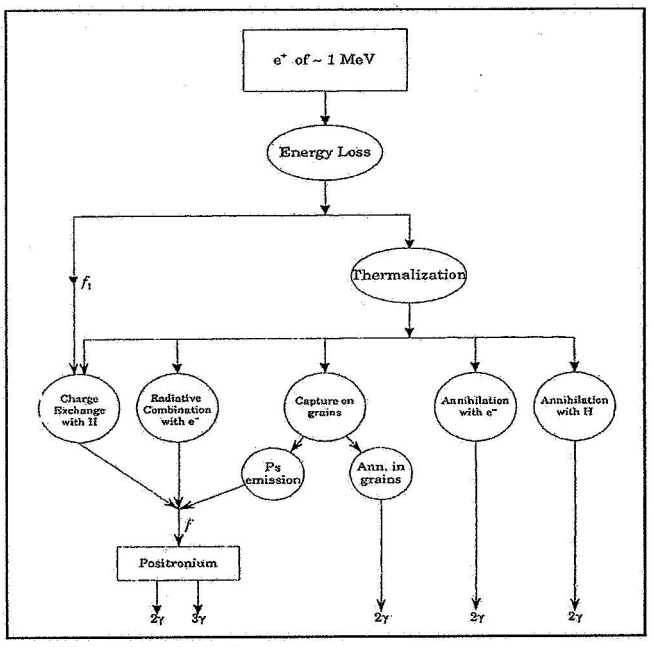

Fig. 12 Annihilation processes.

3.3 Annihilation Processes

Positrons lose energy mainly due to Coulomb collisions, then most of them (> 90%) form positronium in flight. The rest of positrons become thermalized and go into several processes as shown in Fig. 12. Positronium is in either the para or ortho states. Para- positronium (S=0, M_s= 0) decays into two 511 keV photons, and ortho- positronium (S=1, M_s=-1, 0, 1), which forms, 3/4 of the time, undergoes 3-photon decay making continuum below 511keV. (Guessoum et al. 1991)

3.4 **Line Profile** Thermalized e^+ and positronium annihilations create narrow lines, while para-positronium in-flight forms a broad continuum (see Fig. 13). Positrons can migrate from the source and annihilate somewhere in ISM. The 511 keV line profile and positronium fraction are diagnostic of annihilation region. Annihilation probably takes place in warm (T ~ 10^4 K) partially ionized region of ISM. The recent SPI observation using 2004 public data reveals the detection of the broad component (Jean et al., 2005). They fit the line with combination of a narrow line, a broad line, an ortho-positronium continuum, and a power law. Fig. 14 shows the detail. Although the detection was not so significant (3.2σ) with χ^2 ~ 171.3 (dof 148), they find that the broadline flux is about 1/3 of the total 511 keV flux of (1.07±0.03) x 10^{-3} g s^{-1} cm^{-2}, and the positronium fraction is 96.7±2.2 % with the systematic error of ~ 0.2%.

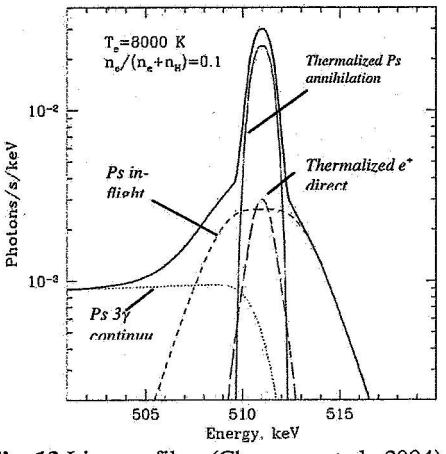

Fig. 13 Line profiles. (Churazov et al., 2004)

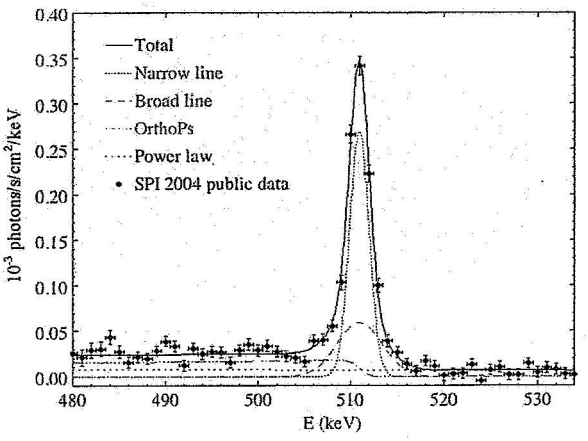

Fig. 14 Detection of the broad line. (Jean et al., 2005)

3.5 Spatial Distribution

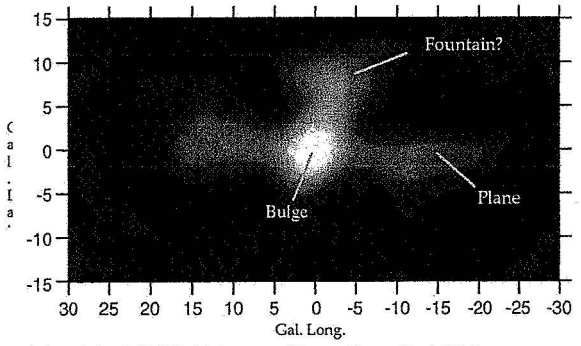

Fig. 15 OSEE 511 map (Purcell et al.,1997)

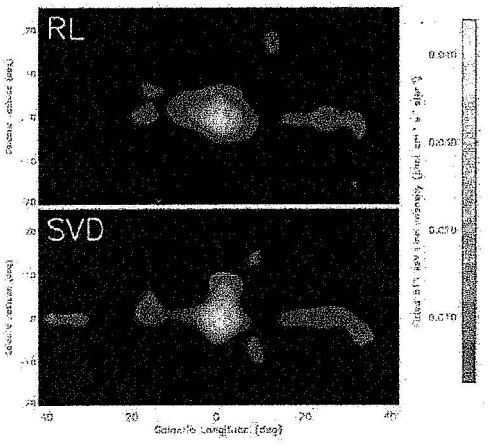

Fig. 16 OSSE/SMM/TGRS map(Milne et al., 2001)

CGRO/OSSE measured the 511 keV distribution, which extends to the high galactic latitude (~ 15°) as well as displaying a strong bulge concentration and emission from the galactic plane (Fig 15, Purcell et al.,1997) The OSSE/SMM/TGRS combined observations using two different algorithms (Richardson-Lucy & Singular Value Decomposition), however, show much less "fountain" (Fig. 16, Milne et al., 2001). Fig. 17 shows the SPI observation. The Bulge distribution data are reasonably well fit by symmetric gaussian with FWHM = 8° ± 1° (Fig. 18). There is no evidence for the OSSE "fountain". Although it could be diffuse, ensemble of point sources cannot be ruled out. The concentration of flux at galactic center suggests that the origins are in the older population.

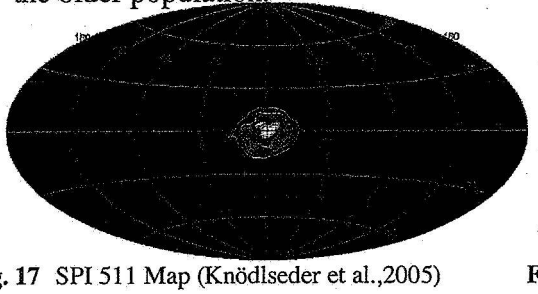

Fig. 17 SPI 511 Map (Knödlseder et al.,2005)

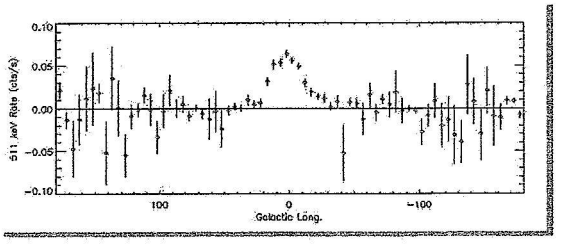

Fig. 18 Symmetric Gaussian (Teegarden et al. 2005)

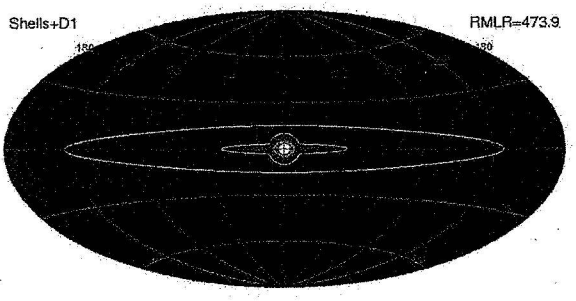

Fig. 19 Bulge + Disk Model (Knödlseder et al.,2005)

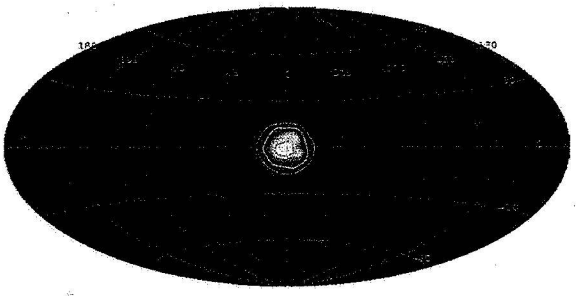

Fig. 20 Positronium Map (Weidenspointner, et al., 2005)

SPI marginally detects the 511 keV galactic disk component at 3-4 σ significance. The result depends on the models we introduce, and Fig. 19 is the best fit model. The 511 keV flux is $F_{511} = (7\pm5) \times 10^{-4}$ cm^{-2} s^{-1}, and the Bulge to the disk flux ratio is 1 – 3. (Knodlseder et al., 2005) A positronium map was also obtained by SPI (Fig. 20). The measurement is more difficult than the 511 keV map due to the broader energy range, the smaller signal-to-background ratio, and more complex background. It has the similar morphology to the 511 keV narrow line, and consistent with the OSSE results. (Weidenspointner, et al., 2005)

3.6 511 keV from ^{26}Al

As we discussed earlier, the distribution of ^{26}Al is concentrated in the galactic disk. It is thought to be produced by nucleosynthesis in massive stars. Thus, the 511 keV disk component could be accounted for by the beta+ decay of ^{26}Al. We estimate the 511 keV flux

$$F_{511} = f_{decay} \times f_{511\,x}\, F_{1809} = 3.5 \times 10^{-4} \text{ cm}^{-2} \text{ s}^{-1},$$

where f_{decay} is the β^+ decay fraction (82%), f_{511} is number of 511 keV photons per annihilation (≈ 0.65), and F_{1809} is the ^{26}Al 1.809 MeV line flux($\approx 7 \times 10^{-4}$ cm^{-2} s^{-1}). Therefore, the predicted 511 keV disk component flux from ^{26}Al decay is ~ 50% of observed value but still within the error bar.

3.8 Searching for Tracer of 511 keV Emission

Fig. 21 shows search for correlations between the 511 keV line emission morphology and tracer maps obtained at various wavelengths. The Reduced Maximum Likelihood-Ratio (RMLR, see Knödlseder et al.,2005) is plotted as function of the tracer. There are strong correlations at nuclear bulge, K and M giant stars, as well as gamma-ray compact objects. RMLR versus the bulge-to-disk (B/D) ratio is shown in Fig. 22. The data favour the large B/D ratio. HEAO-1 traces X-ray binaries, and we know that Low-mass X-ray binaries (LMXBs) have a strong concentration towards the galactic center (B/D ~ 1.8). Candidates for the origin of positrons are LMXBs and old stellar populations such as

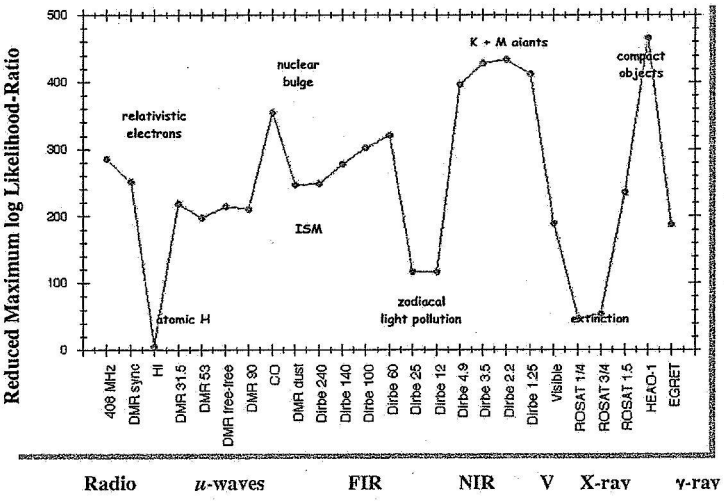

Fig. 21 RMLR as function of the tracer map. (Courtesy of Knödlseder)

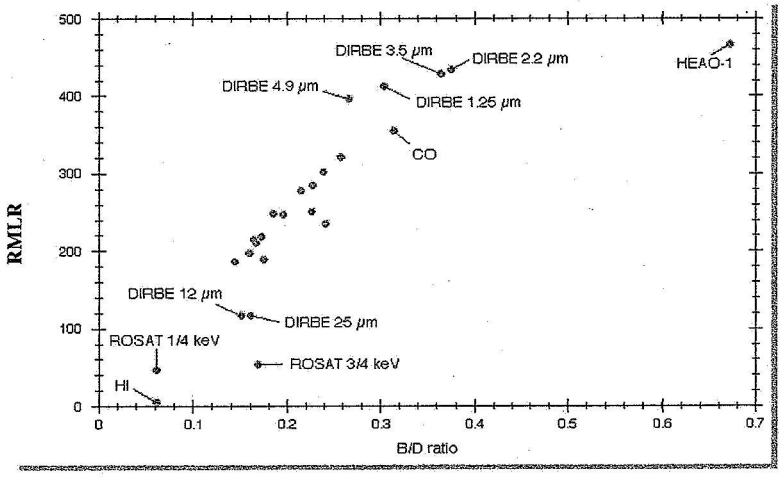

Fig. 22 RMLR as function of the tracer map. (Courtesy of Knödlseder)

Source	*l (deg)*	*b (deg)*	*Distance (kpc)*	*3 σ Flux Limit (10^{-4} ph cm^{-2} s^{-1})*
GX 5-1	*5.08°*	*-1.02°*	*~ 8?*	*< 0.7*
GRS1915+105	*45.37°*	*-0.22°*	*12.5*	*< 1.0*
A 0620-00	*209.96°*	*-6.54°*	*1.5 - 2.5*	*< 3.8*
Nova Muscae	*295.30°*	*-7.07°*	*5.5*	*< 2.0*
Cir X-1	*322.12°*	*0.04°*	*> 8*	*< 1.1*
Cen X-4	*332.24°*	*23.89°*	*?*	*< 1.7*
GX 349+2	*349.10°*	*2.75°*	*?*	*< 0.8*
Sco X-1	*359.09°*	*23.78°*	*0.7*	*< 1.5*

Table 3 511 keV narrow line 3 σ upper flux limits for LMXBs. (Knödlseder et al.,2005)

SNIa. Dark Matter is not ruled out. The 511 keV lines from point sources have been measured by SPI. We, however, find no significant point sources. Table 3 is a summary for LMXBs with 3 σ upper limits.(Knödlseder et al.,2005) An independent, comprehensive line search, using the first year's SPI data, also does not find any 511 keV point sources.(Teegarden & Watanabe 2005)

REFERENCES

Ahn, et al., 2005, PhRvD,71,1301A
Bélanger et al., 2005, astro-ph/0508128
Bildsten, Salpeter & Wasserman, 1993, ApJ, 408,615
Churazov et al., 2004, MNRAS, 357,1377
den Hartog et al., 2004,ATel #293
Diehl et al.,1995, A&A,298L,25
Diehl et al., 2003, A&A,411L,451
Falanga et al., A&A 436, 647, 2005
Guessoum et al.,1991, ApJ, 378, 170
Harris et al., 2005, A&A,433L,49
Jean et al., 2005, astro-ph/0509298
Kappadath, et al. 1996, A&AS, 120, 619
Kinzer, et al., 1997, ApJ, 475, 361
Knödlseder et al.,1999, A&A,345,813
Knödlseder et al.,2005, A&A,441,513
Limongi & Chieffi, 2003, ApJ, 592,L404
Mahoney et al.,1984, ApJ, 286, 578
Malizia et al., 2005, ApJ, 630, L157
Milne et al., 2001, Proceedings of the Fourth INTEGRAL Workshop, 145
Naya et al.,1996, Nature,384,44
Plüschke et al., 2001, Proceedings of the Fourth INTEGRAL Workshop, 55
Prantzos, 2004,A&A,420,1033
Purcell et al.,1997, ApJ,491,725
Sguera et al., astro-ph/0508018
Smith, 2004, Proceedings of the 5th INTEGRAL Workshop, 45
Smith et al., astro-ph/0510658
Teegarden et al., 2005, ApJ, 621, 296
Teegarden & Watanabe, 2005, Submitted to ApJ
Ubertini et al.,2005, ApJ, 629, L109
Watanabe, K., et al., 1997, Proc. of the Fourth *CGRO* Symposium, 1223
Watanabe, et al., 1999, ApJ, 516, 285
Weidenspointner, et al., 2005, Proc. of Semaine de l'Astrophysique Francaise, 471
Zdziarski, et al., 1993, ApJ, 414, L81
Zhang et al.,2004,ApJ,614,37